1

Unbalanced Three-Phase Optimal Power Flow for the Optimization of MV and LV Distribution Grids

Smart distribution grids are developed around the concept of advanced distribution management systems (ADSM), whose features are summarized in this Chapter. Optimal power flow (OPF) techniques are a basic function of ADSM and can be applied effectively for controlling distribution grids at both MV and LV voltage levels. Specialized formulations of OPF need to be developed for defining control actions, such as move tap-ratio in on-load tap changers, switch capacitors or disconnectors, change reference signals or price signals to be sent to prosumers or active end-users. A methodology for controlling active and reactive resources in distribution systems, based on the solution of a three-phase unbalanced OPF, has been proposed and tested in this chapter. Particular attention is devoted to low voltage grids due to their importance. These grids are experiencing dramatic changes in power operations and show the potential to take full advantage of throughout metering and control. Test results showed the feasibility of the approach.

1.1. Advanced distribution management system for smart distribution grids

Smart cities take form around advanced physical infrastructures which, thanks to the pervasive presence of sensors, monitoring, communication systems, and the implementation of optimization and control functions, acquire smartness and improve their overall flexibility, security, reliability and efficiency.

The transformation required for achieving smartness in infrastructures of smart cities appears straightforward when electric power systems are considered. Several

Chapter written by Sergio BRUNO and Massimo LA SCALA.

"smart" functions oriented to the monitoring and control of transmission systems, such as state estimation, topology processor, contingency analysis or dynamic security assessment (DSA), have been customarily in use since the diffusion of control centers and SCADA/EMS in the 1980s. Therefore, a substantial improvement in the smartness of electrical power systems at urban level (basically primary and secondary distribution operating, respectively, at medium voltage MV and low voltage LV level) can be achieved if these same procedures and practices in use for transmission systems were scaled down to distribution.

This basic idea was the principal objective of the earliest formulations of smart distribution networks, usually built around an extensive set of monitoring and control functions embedded centrally in the distribution management system (DMS), or in what it has also been defined as advanced DMS (ADMS). A smart grid, in fact, can be represented with a four-layer structure: the field constituted by physical components (buses, lines, transformers, loads, capacitors, etc.), the set of all measuring and actuating equipment, the ICT layer comprising all communication systems, and the control center (management system) [SAN 10]. The ICT layer is responsible for collecting information about the state of the grid and of its components from sensors, and sending such data to the control center where all evaluations and possible control actions are assessed. Being the place where all data and information are sent to be processed, and where necessary system response are elaborated, the ADMS can be considered the *brain* of a smart distribution grid, being, in other terms, what provides actual intelligence and "smartness" to the grid.

A possible structure of an ADMS was outlined in Fan and Borlase [FAN 09], together with a list of suggested innovative and smart functions to be enabled in distribution systems. ADMS elaborates all available real-time, quasi-real-time and historical data in order to perform management applications that can be performed in a quasi-real-time power system operation framework or in the medium-long term for planning. Based on [FAN 09] and other early literature [HAD 10, MEL 11, MOH 10, MOM 09, ZHA 10], in [BRU 11a], an ADMS architecture for smart distribution systems was outlined (Figure 1.1). The proposed architecture is based on two main control loops starting from the SCADA/ADMS control center. The upper one controls all distribution system-connected devices, including all distributed energy resources (DERs), tap changers and storage facilities, whereas the second loop is interfaced with loads through an advanced metering infrastructure (AMI). SCADA is the core of the proposed architecture: it receives signals from remote terminal units (RTUs) or intelligent electronic devices (IED), such as bay-area controllers, loss-of-mains protection relays, circuit breakers, switching relays and transformers, so that a real-time snapshot of the distribution system can be acquired.

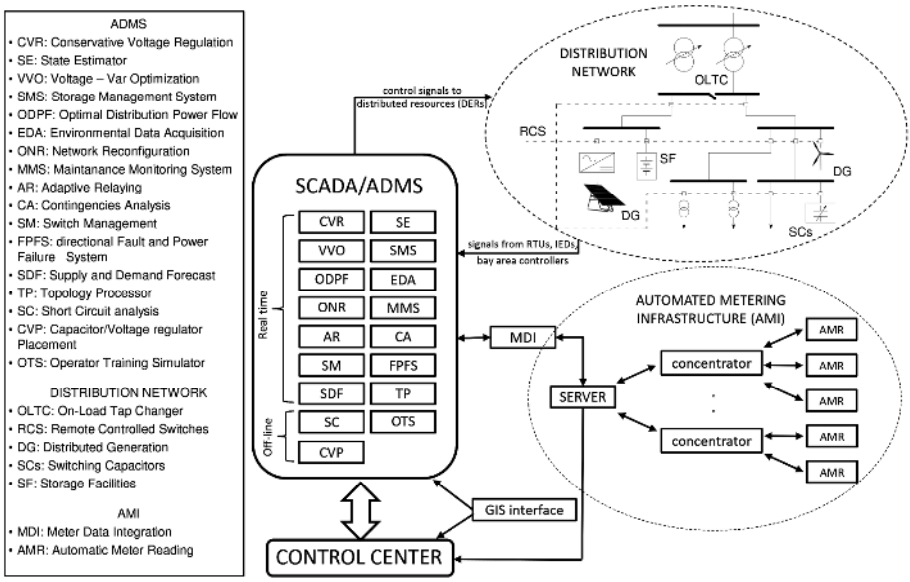

Figure 1.1. *Possible scheme of an ADMS*

It should be noted that control centers and SCADA/DMS platforms had already been often adopted by Distribution System Operators (DSOs) for managing their own networks and performing substation automation and feeder control. However, even when supported by DMS monitoring and remote control functions, power system operation is still characterized by manual procedures that rely on the experience of operators. A full automation of distribution grids is the innovation required for the development of smart networks, and it is based on the presence of bidirectional communication paths between SCADA, control center and power system devices, DERs and, more generally, active customers and prosumers.

Bidirectional communication enables substation automation and supports the enhancement of power system security and reliability through the implementation of smart control functions and through remote control of DERs, at both MV and LV levels. This idea is generally shared by regulators, standardization bodies and network operators, as shown by the most recent normative documents. For example, the draft IEEE Std P1547.8 asserts that DERs must be enabled to respond automatically to variations in grid voltage or following the broadcast of update reference signals or price signals [BAS 15]. This same idea is shared in Europe by other technical standards, for instance [CEI 14, VDE 11], that already define the way LV-distributed generation must contribute to static voltage stability and frequency regulation by means of either local measurements or remote signals. In

the Italian standard [CEI 14] extend this principle to PV generators connected to LV that should be able to receive remote signals with protocol IEC 61850.

If bilateral communication with DERs will be based on modern switchgear equipment and loss-of-mains protection relays, the integration of active customers into SCADA/ADMS passes from the setting up of bilateral communication with Automatic Meter Reading (AMR) devices and Automated Metering Infrastructure (AMI). Unilateral communication, meaning adopting AMR units for mere energy billing purposes, is clearly an incomplete investment that will not lead to the setting up of smart grids.

The case of Italy, which has been the first country in the world to accomplish a massive deployment of smart meters (a penetration of approximately 90% was reached in 2009 [BRU 09]) but still is ranked among the last European countries in terms of actuated demand response schemes [SMA 16], is exemplary. In this specific case, the delay is not only due to the absence of a clear regulatory framework for the development of demand-side auxiliary services, but also due to the rigidity of the proprietary communication systems that have been built primarily for remote metering and billing functions. Non-synchronous electric measures are collected at data concentrators after the polling of AMR devices and then sent off-line to the control center. Bottlenecks are also present on the control center-AMR route, due to a rule system at the server level that automatically assigns priorities to jobs. Control signals to smart meters can be sent only with delays that clearly exceed power system operation time requirements. After about 15 years, a second massive deployment of smart meters (the so-called Smart Meters 2.0) is going to occur in Italy in order to obtain faster communication and response, and provide new functions and services to the final customer.

In all cases where missing links between metering infrastructure and SCADA are present, some technical solutions can be found [ZHA 10]. An interesting solution, presented in [ZHA 10], consists of a middleware named Meter Data Integration (MDI) installed between AMI and SCADA/ADMS (see Figure 1.1). MDI can adapt different AMI communication protocols to the international standards of SCADA and it is potentially able to manage an extremely large quantity of data from meters. This integration could bring many benefits assisting the monitoring and control system in ADMS applications, such as state estimation or supply and demand forecast, and improving management of DERs. The implementation of the MDI block guarantees the integration of SCADA and AMI, also ensuring satisfactory performances in the case of large distribution networks (according to [ZHA 10], such a system might be able to treat a million smart meters in approximately 15 min). Similar solutions can be adopted whenever interoperability issues are experienced due to legacy AMR/AMI.

1.2. Secondary distribution monitoring and control

Setting up all missing downstream and upstream communication links with power system components is not the only significant effort to be made in the way to smart distribution grids. It should be kept in mind that, at the present stage, the entire segment of secondary distribution is very often not monitored nor controlled.

The first approaches to ADMS have considered the sole primary distribution, consumers and producers connected directly at the MV level, but the development of distribution grids for smart cities must necessarily include LV-connected customers and devices in the SCADA/ADMS control schemes. The growing diffusion of small-capacity DERs and the growing demand of demand response (DR) schemes suggest that a much wider number of active users will be willing to participate in the management of the grid shortly. The growth of active users (or prosumers) requires definition and implementation.

The European Distribution System Operators' Association for Smart Grids (EDSO) has recently embraced this idea. This association has recognized the fact that DSOs must become "real" system operators, able to monitor and control power flows and preserve quality of supply at any node of the distribution grid (at both MV and LV levels) as the main objective for the fulfillment of 2020 sustainability targets [MAL 14].

The diffusion of small active users that will be able to respond dynamically to price volatility or to substantial variation in power outputs due to intermittent energy sources can constitute, at the same time, the cause for further system stress and vulnerability, or an opportunity to better control system security and improve system flexibility and efficiency. The key in solving this dilemma is in the ability to monitor and control active users and distributed generation.

It is a matter of fact that keeping distribution systems uncontrolled and managing distribution with the traditional "fit and forget" approach will either affect the power quality and security of the supply or, ultimately, create an insurmountable obstacle for the diffusion of smart green technologies. For example, distributors will not be able to accommodate more distributed generation because of the growing severity of security issues (congestions, voltage rises, unacceptable power quality, etc.). If the "green revolution" and the "smartification" of cities are to occur, electrical grids will have to be able to exploit faster communication channels and an increased number of sensors and control capabilities, enabling the DSOs to monitor and control the distribution grid at any voltage level.

1.2.1. *Monitoring and representation of LV distribution grids*

From a technical point of view, enabling monitoring and control functions in distribution systems appears an achievable target, even though the effort required for the modernization of such systems is huge. This is especially true, for example, in the case of secondary distribution that, presently, is in most cases managed by DSOs more or less like a black box. Very often, primary electrical characteristics, such as voltage and currents profiles, are unknown, except for aggregated data at MV/LV interface. Few measurements are used to represent the state of hundreds of nodes, circuits and end-users that, through secondary distribution, are connected to the primary substation. Load and generation imbalance is generally undetermined at the LV level, and even its modeling is not easy, as the exact location of single-phase objects (loads and generators) is not necessarily known at the central level. In certain cases, such information might not be available at all. This is the case, for example, of single-phase customers in condominiums that were connected to one of the three phases available at the delivery point following just a rotating order. Moreover, LV circuits in secondary distribution require the most frequent maintenance interventions because faults happen more often or because new customers must be accommodated. Circuit modifications are, usually, carried out manually by technicians who keep written notes of changes in the substations and no information of such modifications is transferred back to the control centers. Consequently, very often, an exhaustive and updated database of LV circuit designs and electrical characteristics might not be available at the centralized level.

This means that a specific effort must be made to ensure that LV networks are properly managed and inventoried. Recent studies have focused on the opportunity of employing smart meters and AMI for developing LV grid monitoring and control. The setting up of such functions must deal with several issues due to the complexity of multi-phase unbalanced models, the efficiency and robustness of distribution state estimation (DSE) algorithms, and the relevant number of non-synchronized measurements obtained by the meters.

Traditionally, the problem of DSE has been solved considering statistical models of loads, obtained exploiting available information on load nominal power, types of customers, historical consumption data and load patterns [ROY 93]. More recently, several studies have been aimed at solving specific problems related to distribution systems such as the presence of radial topologies and three-phase unbalanced systems [BAR 95, LU 95], the high resistance to reactance ratio and the very limited number of real-time measurements [BAR 09, SIN 09, WAN 04]. In [SIN 09, WAN 04], it was shown how accurate states of distribution systems can be obtained thanks to the exploitation of smart meters and AMI (pseudo-) measurements. In a few cases, DSE approaches have also been tested on actual LV networks. In [ABD 12], the technical feasibility of adopting smart meters and their instantaneous

measurements (voltage, active and reactive power) for LV network observability and controllability was shown. Similar results were also obtained in [STI 11, STI 13], where data from smart meters have been used for monitoring and controlling voltages in critical nodes [STI 13] and for carrying out semi-automated load flow calculation in 4-wire LV networks [STI 11].

DSOs have already been making an effort to solve the problem of LV network observation. Methods and devices for the auto-detected inventory of LV grids have already been tested [VAR 15]. For example, successful tests were carried out installing a device in secondary substations that identifies the phase and the circuit, where a specific smart meter is physically connected through power line communication (PLC) [VAR 15]. Such results show how, with affordable investments, a complete vision of the LV distribution system is achievable, and that the issue of a correct representation of multi-phase connections can be overcome.

1.2.2. *LV control resources and control architecture*

Another issue to be solved considers the actual availability of devices to be controlled at the LV level. Most pieces of equipment that are currently installed in secondary substations are legacy devices that cannot be adapted for the implementation of smart grids and, in the scenario of *smartification* of LV subsystems, should be necessarily replaced or modified. The clearest example of this is given by the fact that MV/LV transformers are very seldom, if ever, equipped with on-load tap changers (OLTC). Usually MV/LV transformer turns ratios can be adjusted manually through an off-circuit tap changer. This means that any change in turns ratio follows a manual procedure where the transformer has to be put temporarily out of service and customers are not served unless backup auxiliary circuits are available. For obvious reasons, the turns ratio is fixed once at the time of installation, and then changed only when noticeable security issues are experienced by customers (for example, frequent overvoltages due to the proximity of PV generators). The fixed setting of MV/LV tap changer must accommodate voltage profiles for all hours of the day and most seasons.

At present times, end-users themselves constitute legacy, but the growing penetration of household small generation units, batteries, electric vehicles, home automation, heat pumps and smart appliances contributes to forming a vision where all such units will be coordinated, following control signals at local level, or centralized.

DR programs will ensure that distributed control resources are available at the LV level. Theoretically, any electrical appliance might become a control resource. It has been estimated, for example, that about one-third of the overall LV active power

demands are constituted by controllable electrical components [MOK 13]. The list of controllable loads might include not only BESS and EVs, but also private and public lightning systems, and any household electrical machine like washing machines or air conditioning systems, heat pumps and refrigerators. Supposedly, pushing this concept to its limit, any equipment with an inverter-controlled drive might be able to modulate both active and reactive power exchanges.

Utility load management has been discussed and experimented since the 1970s [MOR 79]. In the short term, it is difficult to foresee the development of centralized control of residential appliances, although some hints come from the appliance market. Emblematic is the case of some heat pump manufacturers, which equipped their units with control boards under IEC 61850 protocol for substation automation.

It is rather conceivable that DSOs will be able to send control signals in the form of price signals or energy balance requests that will be accommodated by customers participating in real-time balancing auxiliary services or other demand response schemes. Possible control schemes are usually developed within the *transactive energy* (TE) framework, with TE being "a system of economic and control mechanisms that allows the dynamic balance of supply and demand across the entire electrical infrastructure using value as a key operational parameters" [FOR 16]. Several adoptable control schemes have been presented in [FAR 14] showing how both centralized and decentralized control solutions are viable.

The provision of market services from DERs can be organized aggregating resources in virtual power plants (VPPs) [RAH 16], following, for example, the third-party aggregator experience done at industrial/large tertiary level in the UK Demand Side STOR (Short-Term Operating Reserve) scheme [BAL 15]. Other forms of aggregation could be developed creating a local distribution area (LDA) used by the DSO for the provision of services [KRI 16]. The LDA comprehends the distribution infrastructure and all DERs, aggregators, VPPs and end-users connected at a single primary station or locational marginal price node. This layered optimization framework seems to be appropriate from a technical point of view, as DSO would be able to control and dispatch local resources for load/generation balancing at the transmission-distribution interconnection point, taking into account security and power quality requirements of the whole MV/LV infrastructure below.

1.3. Three-phase distribution optimal power flow for smart distribution grids

In this chapter, a basic methodology for the control of smart distribution grids is shown together with some realistic applications aimed to solve operative problems that might be encountered in distribution systems, at both MV and LV levels. The

methodology hereby presented is based on the formulation of a three-phase distribution optimal power flow (TDOPF) customized for use in distribution grids. The TDOPF methodology aims to optimize control resources in the presence of unbalanced conditions and in the quasi-real-time framework of ADMS. As shown below, the formulation is flexible enough to be applied to different optimization problems and control variables sets.

Optimal power flow (OPF) is the most commonly adopted tool for power system operation and planning. OPF can solve a great number of optimization problems through simple manipulations of objective functions, inequality constraints and control variables, and it is definitely the most flexible tool available for controlling distribution systems in a DMS framework.

Clearly, OPF must be suitably adapted to the evolution of distribution systems and to the new operative requirements. The birth of markets for energy and energy services, the diffusion of public incentive schemes for renewable resources and the growing demand for energy autonomy have all profoundly changed the structure of distribution systems. DSOs must face the new challenges introduced by the pervasive diffusion of distributed generation (DG) that is modifying the way in which distribution grids must be operated. DSOs must enhance distribution capacity, accommodate new generation capacity and satisfy growing load demand and high seasonal peaks, while avoiding expensive reinforcement investments. DSOs must also deal with degraded steady-state conditions, such as strong imbalance, low/high-voltage profiles, reverse power flows and conspicuous deviations of daily chronological demand curves from average profiles. Hence, the definition of TDOPF-based functions, specifically formulated to control the distribution system during its operation, is necessary.

In order to be effective for distributed system operation, TDOPF must respond to several requirements. For example, the formulation and solution of load flow equations must take into account that networks are radial and characterized by high R/X ratios: the adoption of typical decoupled power flow routines is clearly not possible. Moreover, networks must be represented with a full multi-phase representation, allowing the use of 3-wire and 4-wire models and taking into account the possible presence of unbalanced conditions and single-phase components.

Classically, distribution systems have always been unbalanced because of unequal three-phase loads, untransposed lines and conductor bundlings. However, the recent spreading of single-phase DG plants (mostly household photovoltaic panels, but also micro wind generators or micro turbines) has increased the average system imbalance. Given the randomness associated with renewable sources, the level of imbalance is also hardly estimable, raising even more the concern for network security and power quality at both MV and LV levels.

Another necessary requirement for TDOPF is that it must deal with an increased number and variety of available control resources. Control resources can include any kind of DER, such as small generation, storage systems and EVs, DR, power electric devices and inverter-driven machines, disconnector switches, tap changers and switched capacitors. The formulation must therefore be flexible enough to treat sets of heterogeneous control variables.

An example of a TDOPF platform for distribution grids to be employed in an ADMS framework was proposed in [BRO 11, BRU 11b, BRU 12]. A non-exhaustive list of power system operation tools that can be implemented through the SCADA/ADMS architecture is given in Figure 1.1. TDOPF can be suitably formulated to include several (quasi) real-time applications, such as congestion management, voltage-VAr optimization (VVO) or conservative voltage regulation (CVR). All such functions are in fact based on processing data collected at SCADA level and sending back control signals to field devices and actuators (interruptible loads, on-load tap changers, switching capacities, battery management systems, remote controllable switches, etc.). In most cases, the evaluation of optimal control signals can be based on the solution of a TDOPF problem.

The TDOPF methodology proposed in [BRO 11, BRU 11b, BRU 12] was studied for controlling the MV primary distribution grid of a medium-sized town. Given the state of development of AMR/AMI technology on the specific system under study (the secondary distribution of the city of Trani, in Southern Italy), the methodology proposed was developed in order to implement active power load controlling techniques. The main idea was that, through the introduction of special discounted tariffs, the active load of customers could be redispatched in order to fulfill particular operational constraints.

In the proposed architecture, load control signals were sent directly from the control center to households by setting the maximum available loading capacity at AMR level [BRU 11b]. AMR devices are usually able to receive a signal that can change the maximum power which can be consumed. This is usually done remotely in the case of changes in the contracted power (for example, a customer requiring a higher or smaller capacity) or for limiting the maximum power of non-paying customers. The main idea was to adjust this setting dynamically in order to limit the active power demand in specific corridors, using AMR devices as real-time actuators of centralized control.

TDOPF routines can also be employed for VVO, which integrates the problems of voltage regulation and reactive power compensation [BRO 11]. This kind of control is usually performed by means of on-load tap changers and switching capacitors that are manually operated or controlled through local feedback [PAU 11]. In the proposed ADMS framework, set-points of such devices can be

remotely controlled on the basis of TDOPF calculations, according to specific operational targets and aiming to improve voltage profiles across feeders, sustain voltage, reduce losses, improve energy efficiency and conservation.

Clearly, any remote controllable reactive power resource can be integrated in VVO. The idea of employing distributed generation resources (for example, photovoltaic-PV) for local or centralized voltage regulation of smart grids is commonly accepted, even though some issues about control structure (control schemes for local or generalized control) and ancillary services remuneration (PV inverters participating at voltage regulation must be oversized and therefore are more expensive than the ones operating at a fixed power factor) should be still overcome.

The control of voltage profiles can also be aimed at reducing the overall electricity demand, for example, during peaking hours. This practice is usually called conservative voltage reduction (CVR) and can be implemented through the coordinated control of OLTC and reactive resources [BRO 11]. The principle of CVR is to exploit the voltage dependency of loads for curtailing the overall power demand. Loads are not directly shed or curtailed, but they are supplied with voltages lower than the rated ones, but clearly still above the functional bottom limits. This methodology applies very well for peak shaving in residential and tertiary areas, whereas it can be less effective in industrial areas where motors are the bulk component of demand.

1.4. Problem formulation and solving algorithm

1.4.1. *Main problem formulation*

TDOPF mathematical formulations and solutions are similar to the ones adopted for classical single-phase OPF routines [ALS 74, TIN 68]. Both three-phase and single-phase approaches must employ nonlinear optimization techniques. However, the main differentiation concerns the representation of power flow equations. Single-phase OPF is commonly based on the use of the sole positive sequence component model, whereas TDOPF usually adopts sequence or multi-phase models. Moreover, given the need to represent radial networks characterized by high R/X ratios, typical approaches based on decoupled Newton-Raphson load flow codes cannot be employed.

The following formulation, derived by the developments reported in [BRU 11b], has been improved so that faster convergence properties can be achieved, allowing, for example, inclusion of a larger variety of LV control resources and a detailed representation of secondary distribution circuits. The optimization of LV system resources requires special care because a large number of available control resources are expected.

The most compact formulation for TDOPF is given by

$$\min_{\boldsymbol{u}} C_{obj}(\boldsymbol{x},\boldsymbol{u}) \quad [1.1]$$

subject to

$$\boldsymbol{f}(\boldsymbol{x},\boldsymbol{u})=0 \quad [1.2]$$

$$\boldsymbol{g}(\boldsymbol{x},\boldsymbol{u})\leq 0 \quad [1.3]$$

with

$$\boldsymbol{x}\in \Re^n \text{ and } \boldsymbol{u}\in \Re^m$$

where C_{obj} is an objective function, $\boldsymbol{x}$ is the vector of nodal voltages, $\boldsymbol{u}$ is the vector of the m independent control variables, $\boldsymbol{f}$ is the set of load flow equations and $\boldsymbol{g}$ is the set of inequality constraints that usually take into account thermal limits of transformers and lines, power quality or practical limitations on voltage profiles and other functional constraints. As stated before, any formulation of equations $\boldsymbol{f}$ is possible since the proposed method is sufficiently general to consider both full multi-phase and sequence models. The independent variables $\boldsymbol{u}$ are given by active and/or reactive power injected/absorbed by the controlled LV devices (dispatchable loads, DG and PV generators, storage, EV charging pedestals, etc.), or by the controlled set-point of any other devices (for example, the position of an on-load tap changer).

1.4.2. *Application of the penalty method*

The most common approach to treat functional inequality constraints is to apply the penalty method [TIN 68]. This choice leads to the following formulation where inequality constraints [1.3] are transformed into penalty functions to be minimized together with the objective function:

$$\min_{\boldsymbol{u}} C(\boldsymbol{x},\boldsymbol{u}) \quad [1.4]$$

subject to

$$\boldsymbol{f}(\boldsymbol{x},\boldsymbol{u})=0 \quad [1.5]$$

with

$$C(\boldsymbol{x},\boldsymbol{u}) = C_{obj}(\boldsymbol{x},\boldsymbol{u}) + \sum_i C_p^i(\boldsymbol{x},\boldsymbol{u}) \quad [1.6]$$

where C is the overall objective function and C_p^i is the generic i-th penalty function. The only inequality constraints are given by the feasibility domain of control variables:

$$\boldsymbol{u_{min}} \le \boldsymbol{u} \le \boldsymbol{u_{max}} \quad [1.7]$$

In order to take into account the most common operative issues in distribution systems, different penalty functions can be introduced. The inequality constraints introduced here are the ones referred to the thermal limits of branches, the maximum capacity of power transformers and minimum/maximum voltage magnitude.

A possible formulation of the penalty functions in [1.6] is given by

$$C_1 = \sum_{i=1}^{nline} \sum_{p=1}^{nwires(i)} \alpha_{1,i,p} \left(\frac{I_{i,p} - I_{max,i,p}}{I_{max,i,p}} \right)^2 \quad [1.8]$$

with

$$\alpha_{1,i,p} = 0 \quad if \quad I_{i,p} < I_{max,i,p}$$

where $I_{i,p}$ is the current magnitude on the p-th conductor of the i-th branch, $I_{max,i,p}$ is the ampacity of each conductor of the i-th branch, $nwires(i)$ is the number of conductors for the i-th branch and $\alpha_{1,i,p}$ is a weight factor.

$$C_2 = \sum_{j=1}^{ntrasf} \alpha_{2,j} \left(\frac{S_j - S_{max,j}}{S_{max,j}} \right)^2 \quad [1.9]$$

with $\alpha_{2,j} = 0 \quad if \quad S_j < S_{max,j}$

where S_j and $S_{max,j}$ are apparent power and maximum apparent power at the j-th transformer and $\alpha_{2,j}$ is a weight factor;

$$C_3 = \sum_{k=1}^{nbus} \sum_{p=1}^{nwires(k)} \alpha_{3,k,p} \left(\frac{V_{k,p} - V_{lim,k,p}}{V_{lim,k,p}} \right)^2 \quad [1.10]$$

with

$$\begin{cases} V_{lim,k,p} = V_{max,k,p} & if \quad V_{k,p} > V_{max,k,p} \\ V_{lim,k,p} = V_{min,k,p} & if \quad V_{k,p} < V_{min,k,p} \\ V_{lim,k,p} = V_{k,p} & if \quad V_{min,k,p} \le V_{k,p} \le V_{max,k,p} \end{cases}$$

where $V_{k,p}$ is the voltage magnitude referred to the ground at the p-th node of the k-th bus, $V_{min,k,p}$ and $V_{max,k,p}$ are minimum and maximum phase voltage limits and $nwires(k)$ represent the number of nodes and the number of conductors connected to the k-th bus (i.e. two in single-phase circuits, three in three-phase circuits without neutral, four in three-phase circuits with neutral) α_3 is a weight factor.

Please note that the index p, introduced in [1.8] and [1.10], allows inclusion of specific limitations on the fourth wire. This distinction must be made, for example, in all those cases where the neutral wire has a section smaller than the phases, or if neutral voltages must be kept within specific security limits.

1.4.3. *Definition of an unconstrained problem*

The principal assumption for the development of the approach proposed in this chapter is to transform the constrained problems [1.4–1.6] into an unconstrained problem. This assumption is valid through the application of the implicit function theorem, whose conditions are satisfied in a large set of practical cases. Usually, the sole exception is given by operating points close to voltage instability. However, the idea of being close to voltage collapse in a MV or LV network is very far from reality.

Under the Implicit Function Theorem [38] suppose that $\boldsymbol{f}: E^{n+m} \to E^n$ is k times continuously differentiable (C^k-class) function whose mapping domain is T. Suppose that it exists a $(\bar{\boldsymbol{x}}, \bar{\boldsymbol{u}}) \in T'$ $\boldsymbol{f}(\bar{\boldsymbol{x}}, \bar{\boldsymbol{u}}) = 0$ and that the Jacobian with respect to x, $\nabla_x \boldsymbol{f}(\bar{\boldsymbol{x}}, \bar{\boldsymbol{u}})$, is not singular. Then there exists a neighbourhood of $\bar{\boldsymbol{u}}$, $N(\bar{\boldsymbol{u}}) \subset E^m$ and a unique function $\boldsymbol{\gamma} \in C^k[N(\bar{\boldsymbol{u}})], \boldsymbol{\gamma}: N(\bar{\boldsymbol{u}}) \to E^n$ with $\boldsymbol{\gamma}(\bar{\boldsymbol{u}}) = \bar{\boldsymbol{x}}$ and $\boldsymbol{f}(\boldsymbol{\gamma}(\bar{\boldsymbol{u}}), \bar{\boldsymbol{u}}) = 0$ for all $\bar{\boldsymbol{u}} \in N(\bar{\boldsymbol{u}})$.

Under the conditions given by this theorem, it is possible to assume the existence of a unique function $\boldsymbol{\gamma}(\bar{\boldsymbol{u}}) = \bar{\boldsymbol{x}}$ that allows reformulation of the constrained

problem [1.4–1.6] into an unconstrained problem, in the neighborhood of the solution of the load flow equations $(\bar{\boldsymbol{x}}, \bar{\boldsymbol{u}})$. The optimization problem then becomes:

$$\min_{\boldsymbol{u}} C(\boldsymbol{\gamma}(\boldsymbol{u}), \boldsymbol{u}) \qquad [1.11]$$

with

$$\boldsymbol{u}_{min} \leq \boldsymbol{u} \leq \boldsymbol{u}_{max}$$

The solution of this problem [1.11] can then be found imposing the conditions

$$\nabla \boldsymbol{C} = \left[\frac{\partial C}{\partial u_1} \quad \frac{\partial C}{\partial u_2} \quad \cdots \quad \frac{\partial C}{\partial u_m} \right]^{\mathrm{T}} = 0 . \qquad [1.12]$$

1.4.4. *Application of a quasi-Newton method*

In order to solve [1.12], having chosen an initial value of the control variable vector $\boldsymbol{u}_0$, the Newton method can be applied iteratively through the rule

$$\boldsymbol{u}_{k+1} = \boldsymbol{u}_k - \boldsymbol{H}_k^{-1} \cdot \nabla \boldsymbol{C}_k \qquad [1.13]$$

where the Hessian matrix $\boldsymbol{H}_k$ and the gradient $\nabla \boldsymbol{C}_k$ are calculated at the generic *k*-th iteration. Typically, the iterative solution of equations [1.12] through [1.13] requires the calculation of the inverse matrix $\boldsymbol{H}_k^{-1}$ at each iteration *k*. If the size of the problem is large, as in a realistic-sized network where a large number of control variables must be taken into account, the computational burden required for calculating the second derivatives and the inverse Hessian matrix might be too heavy, comparing with ADMS time requirements. For this reason, in the proposed approach a quasi-Newton method is applied, allowing approximation of the value of the Hessian matrix and of its inverse at each iteration *k*, through some simple calculations (mostly matrix multiplications and sums). This approach significantly reduces the time necessary for solving each iteration, as the only time consuming routine left is the evaluation of sensitivities $\nabla \boldsymbol{C}_k$.

The application of quasi-Newton methods to the solution of [1.12] requires the iterative update of control variables according to the rule:

$$\boldsymbol{u}_{k+1} = \boldsymbol{u}_k + \alpha_k \cdot \boldsymbol{p}_k \qquad [1.14]$$

where α_k is the step-length, and the direction $\boldsymbol{p}_k$ is given by

$$\boldsymbol{p}_k = -\boldsymbol{B}_k^{-1} \cdot \nabla \boldsymbol{C}_k \qquad [1.15]$$

and $\boldsymbol{B}_k$ is the Hessian matrix approximation at the iteration k and $\boldsymbol{B}_k^{-1}$ is its inverse.

At the end of each iteration k, the inverse $\boldsymbol{B}_{k+1}^{-1}$ is evaluated, according to the chosen solving method, through a formula that can be represented generically as a function

$$\boldsymbol{B}_{k+1}^{-1} = h\left(\boldsymbol{B}_k^{-1},\ \boldsymbol{y}_k, \boldsymbol{s}_k\right) \qquad [1.16]$$

where $\boldsymbol{s}_k = \boldsymbol{u}_{k+1} - \boldsymbol{u}_k$ and $\boldsymbol{y}_k = \nabla \boldsymbol{C}_{k+1} - \nabla \boldsymbol{C}_k$.

One the simplest formulations of [1.16] is given by the expression:

$$\boldsymbol{B}_{k+1}^{-1} = \lambda_{k+1} \cdot \boldsymbol{I}_m \qquad [1.17]$$

where λ_{k+1} is a scalar suitably chosen on the basis of computational and convergence properties and $\boldsymbol{I}_m$ is the m-dimensional identity matrix. Several formulations have been proposed for the evaluation of λ_{k+1} [BRE 03]. A suitable choice is given by the method proposed by Barzilai and Borwein [BAR 88, BRE 97], where

$$\lambda_{k+1} = \frac{\boldsymbol{y}_k^{\,T} \boldsymbol{s}_k}{\boldsymbol{y}_k^{\,T} \boldsymbol{y}_k} \qquad [1.18]$$

This methodology is appropriate whenever the computational cost of each iteration is negligible with respect to the overall algorithm or if the problem is characterized by good convergence properties (minor nonlinearities, convexity, etc.).

If the problem requires more robustness or faster convergence, other methods based on a formulation of $\boldsymbol{B}_{k+1}^{-1}$ as a full matrix can be adopted. The most common formulas adopted for evaluating [1.16] are given by the BFGS (Broyden, Fletcher, Goldfarb and Shanno), the DFP (Davidon, Fletcher and Powell) and symmetric rank 1 (SR1) methods [NOC 06]:

$$\text{(BFGS)} \qquad \boldsymbol{B}_{k+1}^{-1} = \left(\boldsymbol{I} - \frac{\boldsymbol{s}_k \boldsymbol{y}_k^{\mathrm{T}}}{\boldsymbol{y}_k^{\mathrm{T}} \boldsymbol{s}_k}\right) \cdot \boldsymbol{B}_k^{-1} \cdot \left(\boldsymbol{I} - \frac{\boldsymbol{y}_k \boldsymbol{s}_k^{\mathrm{T}}}{\boldsymbol{y}_k^{\mathrm{T}} \boldsymbol{s}_k}\right) + \frac{\boldsymbol{s}_k \boldsymbol{s}_k^{\mathrm{T}}}{\boldsymbol{y}_k^{\mathrm{T}} \boldsymbol{s}_k} \qquad [1.19]$$

$$\text{(DFP)} \qquad \boldsymbol{B}_{k+1}^{-1} = \boldsymbol{B}_k^{-1} - \frac{\boldsymbol{B}_k^{-1}\boldsymbol{y}_k\boldsymbol{y}_k^{\mathrm{T}}\boldsymbol{B}_k^{-1}}{\boldsymbol{y}_k^{\mathrm{T}}\boldsymbol{B}_k^{-1}\boldsymbol{y}_k} + \frac{\boldsymbol{s}_k\boldsymbol{s}_k^{\mathrm{T}}}{\boldsymbol{y}_k^{\mathrm{T}}\boldsymbol{s}_k} \qquad [1.20]$$

$$\text{(SR1)} \qquad \boldsymbol{B}_{k+1}^{-1} = \boldsymbol{B}_k^{-1} + \frac{\left(\boldsymbol{s}_k - \boldsymbol{B}_k^{-1}\boldsymbol{y}_k\right)\cdot\left(\boldsymbol{s}_k - \boldsymbol{B}_k^{-1}\boldsymbol{y}_k\right)^{\mathrm{T}}}{\left(\boldsymbol{s}_k - \boldsymbol{B}_k^{-1}\boldsymbol{y}_k\right)^{\mathrm{T}}\boldsymbol{y}_k} \qquad [1.21]$$

Among the three methods, BFGS is considered the most efficient. BFGS has very effective self-correcting properties, whereas it is recognized that the DFP method is less successful in correcting bad Hessian approximations. Please note that the self-correcting properties of BFGS are ensured only if an adequate line search is performed. The formulation of the SR1 method in [1.21] does not guarantee that its denominator is non-singular. For such reason, BFGS is usually preferred unless specific algorithms are employed in order to avoid the SR1 method leading to numerical instability or breakdown. However, all three methods belong to the Broyden class of quasi-Newton updating formulas and, theoretically, they would yield the same Hessian approximation (and therefore the same iterates), provided that an exact linear search of α_k is made [NOC 06].

Clearly, an exact linear search of α_k is not always performed because it requires the solution of another optimization problem. In this specific case, it would require the computation of the same second derivatives that we wanted to avoid. Generally, good convergence properties, and better chances to reach the global minimum, are achieved if the two Wolfe conditions are respected.

The solution $\hat{\boldsymbol{u}}_{k+1} = \boldsymbol{u}_k + \hat{\alpha}_k \cdot \boldsymbol{p}_k$, obtained with a generic $\hat{\alpha}_k$, fulfills, respectively, the first Wolfe condition of sufficient decrease if

$$C\left(\hat{\boldsymbol{u}}_{k+1}\right) \le C\left(\boldsymbol{u}_k\right) + \mathrm{c}_1 \cdot \hat{\alpha}_k \cdot \nabla \boldsymbol{C}_k^{\mathrm{T}} \cdot \boldsymbol{p}_k \qquad [1.22]$$

The second Wolfe condition, or curvature condition, is satisfied if

$$\nabla \hat{\boldsymbol{C}}_{k+1}^{\mathrm{T}} \cdot \boldsymbol{p}_k \ge \mathrm{c}_2 \cdot \nabla \boldsymbol{C}_k^{\mathrm{T}} \cdot \boldsymbol{p}_k \qquad [1.23]$$

with

$$0 < \mathrm{c}_1 < \mathrm{c}_2 < 1 .$$

Even though both conditions should be satisfied for defining the most suitable step-length, in certain cases it might be convenient to consider the first condition

only. Checking the second Wolfe condition requires the evaluation of the gradient $\nabla \hat{\boldsymbol{C}}_{k+1}$. If the computational burden associated with the calculation of this gradient is high, it might be more efficient to accept a step-length that satisfies only the first condition, slowing the overall convergence behavior (the number of iterates) but decreasing the time necessary for each iterate.

In the proposed approach, derivatives are calculated numerically. Therefore, it is rather convenient to consider only the first Wolfe condition instead of running the time-consuming sensitivity analysis procedure multiple times. This can be done if the line-search chooses the candidate step-length appropriately. The algorithm applied in this approach for the evaluation of the step-length is based on the iterative procedure, based on quadratic and cubic interpolation proposed in [NOC 06] and not reported here for the sake of brevity. This approach takes into account the sole sufficient decrease condition [1.22]. According to the common practice, the initial step-length can be set to 1 and c1 is chosen sufficiently small (for example, 10^{-4}).

1.4.5. *Solving algorithm*

The structure of the solving algorithm is shown in Figure 1.2. The method starts with an initial guess of $\boldsymbol{u}_0$ that is used to evaluate the first set of sensitivities. As quasi-Newton methods calculate the inverse Hessian approximation based on the last two iterations, the algorithm requires an initialization and a first guess of the Hessian matrix. The common practice is to assume $\boldsymbol{Q}_0$ is equal to the identity matrix.

The gradient $\nabla \boldsymbol{C}_k$ is calculated as proposed in [BRU 11b] through numerical partial derivatives of C, calculated applying, one at a time, a small deviation on control variables and observing the variation of C around the initial solution of the three-phase distribution load flow (DLF) for $\boldsymbol{u}_k$.

At the generic k-th iteration, the control variable vector is updated moving the solution along the search direction $\boldsymbol{p}_k$ with an optimal step-length α_k. The algorithm stops whenever the sensitivities drop below a prefixed tolerance level ($\|\nabla \boldsymbol{C}_{k+1}\| \leq \varepsilon$).

The algorithm was implemented on a Matlab-OpenDSS platform based on a two-way data exchange between a Matlab code that evaluates sensitivities and assesses control variable variations, and the OpenDSS simulation engine that performs DLF and updates the network model following the control variable variations evaluated by the optimization routines. OpenDSS is an open-source software, developed by EPRI that has been designed specifically for solving distribution circuits and has recently established itself as a standard in smart grids analysis and planning.

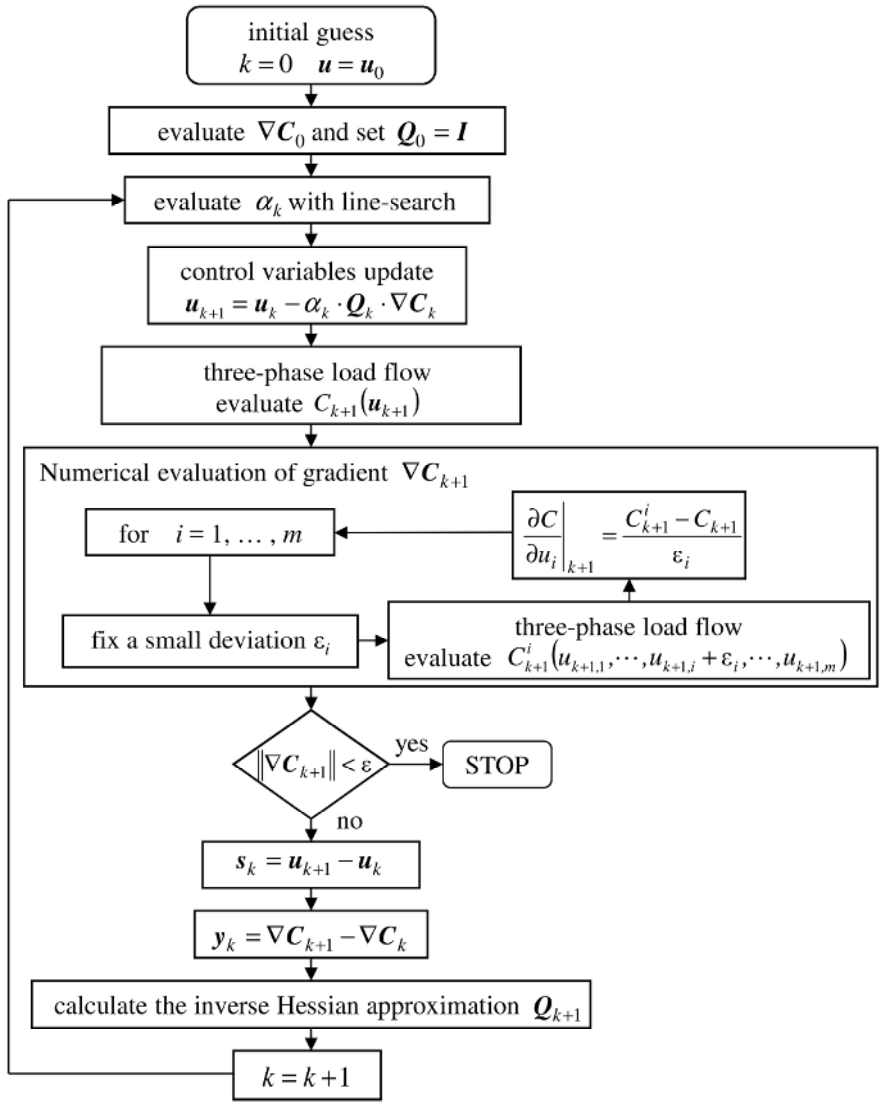

Figure 1.2. *Flow-chart of the proposed algorithm*

The two codes communicate by means of the COM interface that is available in the OpenDSS software package [HTT]. The COM interface makes it possible to use a code already written and optimized by someone else (in this case OpenDSS) in

one's own programming environment (Matlab). This is an important feature because it allows exploitation of the perks of a well-structured DLF engine, specifically optimized and compiled for solving, in fractions of a second, complex distribution networks characterized by radial configuration and high R/X ratios.

The adoption of the OpenDSS DLF engine also allows treatment of any type of electric device easily and includes a large variety of control resources. The network model, in fact, is implemented with a structure that is different with respect to the classical nodal structure used in the IEEE Common Data Format. Each device is modeled as an object that is connected to a certain number of single-phase nodes; nodes are then connected by branches and wires. This means that any multi-phase device, being, for example, a single-phase or three-phase load or generator, can be easily connected to any system bus. Each object can have its own characteristics so, for example, differently for any classical nodal approach, an indefinite number of loads, each one characterized by its own model (number of phases, voltage dependence, ZIP model, etc.), can be connected to the same bus and then univocally monitored or controlled.

The proposed hybrid platform makes it possible to respond to the specific TDOPF requirements that were introduced beforehand. The choice of using OpenDSS relies on the advantages already listed and, of course, on its "open source-ness". However, any other DLF software, being a commercial or research product, is compatible with the proposed architecture, provided that an efficient data exchange interface is available.

1.5. Application of the proposed methodology to the optimization of a MV network

The test results presented in this section were obtained implementing the proposed algorithm on a realistic sized representation of the urban distribution network managed by a DSO (AMET-Trani) that supplies energy for a medium-sized city in the South of Italy (about 50,000 inhabitants, 35,000 customers, and a municipal area of approximately 100 km^2). The system was modeled considering all HV and MV elements. The model is composed of two 150 kV/20 kV transformers equipped with controllable tap changers, eleven 20 kV feeders, 900 buses, 1,000 distribution lines (cabled and overhead), 100 controllable switches and 500 load buses. A simplified scheme of the distribution substation is given in Figure 1.3, whereas a planimetric map of the modeled urban network is given in Figure 1.4.

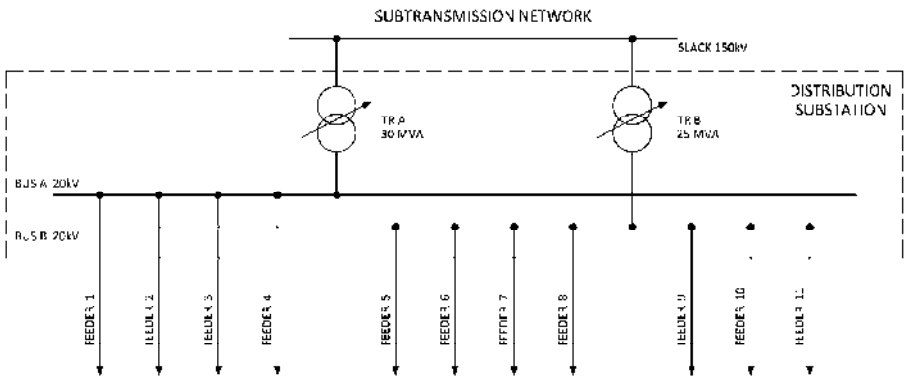

Figure 1.3. *Simplified scheme of the AMET primary substation*

Figure 1.4. *Planimetry of the AMET urban distribution network. For a color version of the figure, see www.iste.co.uk/lascala/smart.zip*

Table 1.1 shows the rated power and current of a MV feeder supplied by the two HV/MV transformers. The maximum current is given by the threshold of overcurrent protection devices.

Feeder #	Transformer	Rated voltage [kV]	Rated current [A]	Rated power [kVA]
1	TRA	20	187	6,470
2	TRA	20	187	6,470
3	TRA	20	187	6,470
4	TRA	20	187	6,470
5	TRB	20	85	2,940
6	TRB	20	104	3,600
7	TRB	20	85	2,940
8	TRB	20	187	6,470
9	TRB	20	85	2,940
10	TRB	20	128	4,430
11	TRB	20	128	4,430

Table 1.1. *Main data of 20 kV feeders*

The distribution system is radial and each node is supplied by a single feeder only. The configuration of the network can be modified, changing the state of some controllable switches, which, according to normal operational procedures, are fixed. The topology does not change unless significant disturbances are experienced (a permanent fault, for example) or unless maintenance works require energizing a branch through another route.

In this section, secondary distribution circuits and MV/LV transformers have been neglected. LV elements are therefore not represented. Loads are modeled through equivalents at MV level. In this case, the system was represented under balanced conditions, assuming that aggregated loads are more or less balanced at MV level.

The base case was obtained considering the actual operating conditions registered at noon on the third Wednesday of December 2009. In such conditions, the system supplied approximately 35 MW by means of the two 150/20 kV transformers located at the substation. The first 30 MVA transformer (TRA) carried approximately 21.5 MVA supplying energy for four urban feeders. The remaining seven feeders were supplied by a 25 MVA transformer (TRB) for a total amount of 11.3 MVA.

Test cases were obtained considering the inputs of the largest distributed generation units directly connected at MV level (Table 1.2) and modifying the overall loading level.

Generator #	1	2	3	4	5	6	7
Rated power [kW]	1,000	2,000	1,000	1,000	4,000	1,000	1,000
Feeder #	1	2	4	10	5	5	5
Generator #	8	9	10	11	12	13	
Rated power [kW]	1,000	1,000	1,000	3,000	1,000	3,000	
Feeder #	6	8	8	8	9	9	

Table 1.2. *Distributed generation in the test system*

1.5.1. *Case A: optimal load curtailment*

The first case was aimed at assessing load control in order to eliminate congestions on the HV/MV power transformers and distribution feeders. This base case was modified assuming the occurrence of a uniformly distributed load increase of 50%. The base case was also modified considering that the generators in Table 1.2 (mostly PV units) are producing approximately 20% of their nominal power. Having run a load flow with this model, the result is that the transformer TRA is overloaded and the feeders #1, #3, #4 and #6 are congested.

Overloads and congestions can be cleared through the solution of the proposed TDOPF problem, adopting the penalty functions introduced in [1.8–1.10] and introducing an objective function aimed at minimizing the amount of load to be curtailed or shed:

$$C_0 = \sum_{i=1}^{nloads} \alpha_0 \left(\frac{u_i - u_i^0}{u_i^0} \right)^2 \qquad [1.24]$$

where *nloads* is the total number of curtailable loads, u_i is the active load power of the *i*-th load, and α_0 is a weighting factor.

As the primary concern is to study the performance of the proposed algorithm and assess the required computational effort, the optimization problem was solved considering that curtailable loads can be found at each load bus (more than five hundreds). This means that the number of control variables is equal to the number of loads (*nloads* is equal to 505). Consequently, the evaluation of the gradient through the numerical evaluation of the derivatives requires the solution of more than 500 distribution load flows.

The algorithm converged in 11 iterations (see Table 1.3), reaching an optimal solution where all penalty functions are null. In Table 1.4, it is possible to follow how main constrained variables vary along the iterative process. As shown in Table 1.4, before control at iteration 0, feeders #1, #3, #4, and #6 were congested. Moreover, the transformer TRA, supplying power to the first four feeders, was overloaded.

iter #	C_0[p.u.]	C_1 [p.u.]	C_2 [p.u.]	C_3 [p.u.]	C (tot) [p.u.]
0	0.0000	0.6705	0.0641	0.0000	0.7346
1	0.0000	0.6643	0.0632	0.0000	0.7275
2	0.0018	0.1174	0.0000	0.0000	0.1354
3	0.0018	0.0575	0.0000	0.0000	0.0593
4	0.0022	0.0001	0.0000	0.0000	0.0023
5	0.0023	0.0000	0.0000	0.0000	0.0023
…	…	…	…	…	…
10	0.0019	0.0000	0.0000	0.0000	0.0020
11	0.0019	0.0000	0.0000	0.0000	0.0019

Table 1.3. *Case A: convergence behavior of the TDOPF*

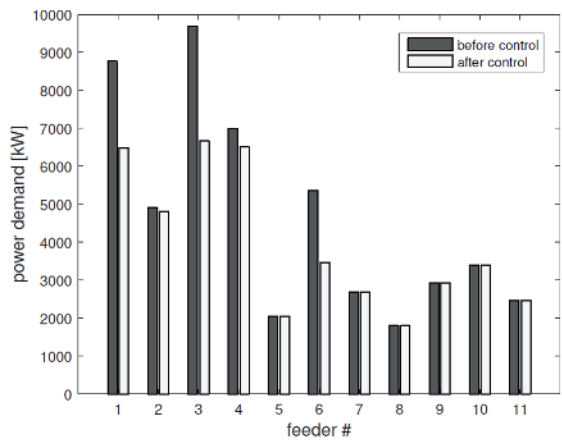

Figure 1.5. *Case A: overall power demand at each feeder (before and after control)*

The optimal load curtailment evaluated through the TDOPF is characterized by a load reduction of approximately 7,800 kW (8.4% of the overall requested active power). The distribution of load curtailment among feeders is shown in Figure 1.5. It can be seen how loads supplied by feeders #5, #7, #8, #9, #10 and #11 were unaffected by the control. Currents flowing in such feeders (see Table 1.3) are also unchanged (just some minor changes due to the voltage adjustments). As expected, the greatest curtailment was experienced by loads supplied by the congested feeders #1 and #3, which also contribute to the overload of transformer TRA.

Iter #	S_1 [kVA]	S_2 [kVA]	I_1 [A]	I_2 [A]	I_3 [A]	I_4 [A]	I_5 [A]	I_6 [A]	I_7 [A]	I_8 [A]	I_9 [A]	I_{10} [A]	I_{11} [A]
0	32,402	19,891	252.28	146.27	273.65	200.57	36.27	163.62	79.29	25.87	52.87	104.05	77.69
1	32,384	19,877	252.11	146.25	273.43	200.48	36.28	163.21	79.30	25.87	52.87	104.05	77.69
2	29,496	17,811	224.59	143.02	238.89	186.58	36.96	102.86	79.92	26.43	53.78	104.95	78.30
3	28,546	17,844	213.57	143.34	223.10	187.32	36.97	103.49	79.93	26.44	53.81	104.97	78.32
4	26,040	17,927	187.03	143.21	186.01	187.49	37.02	105.10	79.98	26.48	53.87	105.03	78.36
5	26,046	17,821	187.22	143.23	186.22	187.20	37.05	102.05	80.00	26.50	53.91	105.07	78.39
…	…	…	…	…	…	…	…	…	…	…	…	…	…
10	26,083	17,896	187.20	143.31	187.28	187.11	37.03	104.23	79.98	26.48	53.88	105.04	78.36
11	26,083	17,895	187.21	143.32	187.26	187.11	37.03	104.21	79.98	26.48	53.88	105.04	78.36

Table 1.4. *Case A: main variables along the iterative process*

1.5.2. *Case B: conservative voltage regulation*

In this second test, the proposed TDOPF was applied to the CVR problem. The aim of this optimization is to minimize the consumption of active power by reducing voltage levels as much as possible. Voltages should never go below a certain level because they might cause malfunctioning of electric appliances or undesired triggering of protection relays. It is reasonable to accept that voltage magnitude at MV level should be kept above the value 0.95 p.u. Theoretically, even lower voltage levels can be accepted for short time periods, but, in the simulations, the bottom limit was set prudentially to 0.95, so that a few percent voltage drop in LV circuits is still possible.

CVR bases its efficacy on the voltage dependency of loads. Clearly, if loads are modeled with a constant active power model, no real benefit can be gained from CVR. In order to make credible assumptions with regard to the average nature of aggregated loads connected to MV in residential areas, the following general load distribution has been assumed: approximately 50% fixed impedance model, 25% constant active power and quadratic reactive (somewhat like a motor) and 25% linear active power and quadratic reactive (mixed resistive/motor). The loads at each node were decomposed into three equivalent loads following this statistic. Having used an object-oriented system representation, this step is very easy, as any number of loads, and of any species (for example three-phase or single-phase loads characterized by any ZIP model), can be added at any system bus without much effort.

A possible formulation of this problem is obtained by introducing an objective function aimed at minimizing the quantity of active power supplied to the network:

$$C_0 = \min_{u} \sum_{j=1}^{ntrasf} \alpha \left(\frac{P_j}{P_j^0} \right)^2 \qquad [1.25]$$

where P_j is the active power carried by the j-th HV/MV transformer, and P_j^0 is the initial active power. Please note that this formulation is possible as long as the transformers are transferring energy from the HV grid to the MV. If reverse power flows are experienced, this formulation is no longer valid. However, it would be rather peculiar that CVR was performed when the distribution system has already been exporting energy.

The objective function [1.25] is minimized together with the penalty functions already introduced in [1.8–1.10]. V_{min} and V_{max} in [1.10] are set, respectively, to 0.95 and 1.05 p.u. The set of control variables $\mathbf{u}$ is given by the voltage reference signals of OLTC and the reactive power output of the DG units.

Please note that tap changers can assume only a few discrete positions; usually 33 steps from −16 to +16 that correspond to equivalent ratios in the interval 0.9–1.1 p.u. For this reason, the problem should be treated as a mixed integer nonlinear problem (MINLP). However, given the small number of discrete variables, this problem can be more easily solved through decomposition techniques or by relaxing the integer variables. The latter scheme, utilized in the proposed code, is based on the assumption of the tap ratio as a continuous variable; the continuous value evaluated during the iterative process is then approximated to the nearest discrete step.

The solution, obtained after seven iterations as shown in Table 1.5, is characterized by an acceptable voltage profile (no lower limit violations) with an overall active power decreased from 31.7 MW to 27.0 MW with an active power reduction of almost 15%. In Figure 1.6, it can be observed how the voltage level at all nodes has been decreased but no minimum voltage violations are present. The control of reactive resources was minimum, given the much lower sensitivity shown by these resources with respect to the other control variables (transformer equivalent turns ratio).

iter #	C_0 [p.u.]	C_1 [p.u.]	C_2 [p.u.]	C_3 [p.u.]	C(tot) [p.u.]	P_1 [kW]	P_2 [kW]	Tap position TRA	Tap position TRB
0	1.0000	0.0000	0.0000	0.0000	1.0000	21.286	10.459	2	4
1	1.0000	0.0000	0.0000	0.0000	1.0000	21.286	10.459	2	4
2	0.9721	0.0000	0.0000	0.0000	0.9721	21.027	10.293	1	3
3	0.9148	0.0000	0.0000	0.0000	0.9148	20.773	9.796	0	0
4	0.7851	0.0000	0.0000	0.0000	0.7851	20.013	8.665	−3	−7
5	0.5543	0.0000	0.0000	41.6989	42.2532	16.816	7.281	−16	−16
6	0.6689	0.0000	0.0000	3.8387	4.5076	16.800	8.844	−16	−6
7	0.6819	0.0000	0.0000	3.8514	4.5333	16.798	9.004	−16	−5
8	0.6819	0.0000	0.0000	3.8520	4.5339	16.798	9.004	−16	−5
9	0.7277	0.0000	0.0000	0.0000	0.7277	18.005	8.997	−11	−5

Table 1.5. *Case B: convergence behavior of the TDOPF and main variables*

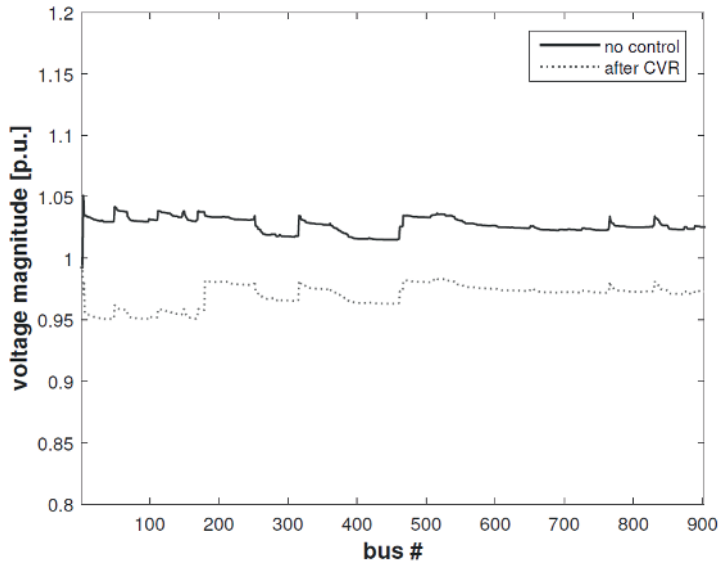

Figure 1.6. *Case B: voltage profiles before and after control*

1.5.3. *Case C: voltage rise effects*

An approach similar to that proposed in the previous case can be adopted for eliminating steady-state voltage rise effects caused by the inversion of flow on distribution lines due to excessive DG production. The case studied in this section was created by considering that each of the DG units in Table 1.2 is producing approximately 80% of its nominal power. In addition, load profiles were altered considering a 30% load decrease with respect to the base case. As a result, the energy flow in the second transformer TRB is reversed (from MV to HV). This condition can be dangerous because it causes a voltage rise in several nodes of the network.

In the specific network under study, for example, this condition is typical for the rural feeders, where energy consumption can be very low in certain hours of the day and in certain seasons, and where the largest PV farms have also been installed. Reverse power flows are experienced in these feeders because most of the loads are linked to agriculture activities that, in central hours of summer days when PV farms reach their seasonal production peak, are characterized by very low consumption; fields, in fact, cannot be irrigated in sunny hours or when the temperature is too high. This is just an example of operating conditions that can cause reverse power flows but, clearly, with the growing penetration of DG, reverse power flows are expected to be experienced more and more frequently on MV distribution feeders.

In order to control voltages and force them back to acceptable levels (i.e. below the 1.05 p.u. limit), a TDOPF was formulated considering the penalty functions [1.8–1.10] and a generic objective function aimed at reducing the control effort:

$$C_0 = \sum_{i=1}^{m} \alpha_0 \left(\frac{u_i - u_i^0}{u_i^{max} - u_i^{min}} \right)^2 \qquad [1.26]$$

where m is the number of control variables. For this simulation, the set of control variables u is given by the voltage reference signals of OLTC and the reactive power output of the DG units. V_{min} and V_{max} in [1.10] are set, respectively, to 0.95 and 1.05 p.u.

In Figure 1.7, it is shown how voltage magnitude was exceeding the upper limit for certain buses in proposed operating conditions and how such violations are not experienced anymore after control is applied. Clearly, the voltage profiles of all nodes supplied by the transformer TRA are unchanged since no control on the tap position was necessary (Table 1.6). Furthermore, it can be observed that, in the tested case, the reactive control was negligible with respect to the contribution of tap-changer adjustments, as the latter were more sensitive.

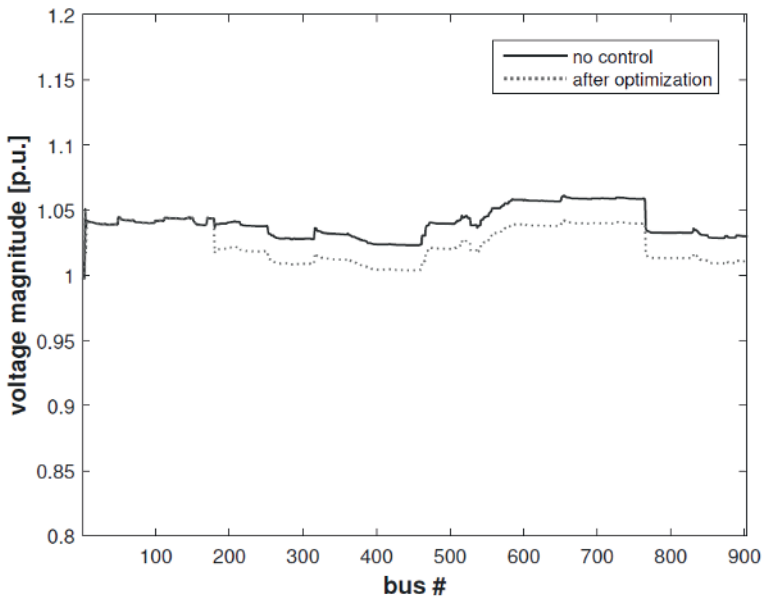

Figure 1.7. *Case C: voltage profiles before and after control*

iter #	C_0 [p.u.]	C_1 [p.u.]	C_2 [p.u.]	C_3 [p.u.]	C(tot) [p.u.]	tap position TRA	tap position TRB
0	0.0000	0.0000	0.0000	0.3973	0.3973	0	1
1	0.1129	0.0000	0.0000	0.0000	0.1129	0	−16
2	0.0879	0.0000	0.0000	0.0000	0.0879	0	−14
3	0.0063	0.0000	0.0000	0.0000	0.0063	0	−3
4	0.0035	0.0000	0.0000	0.0000	0.0035	0	−2
5	0.0035	0.0000	0.0000	0.0000	0.0035	0	−2

Table 1.6. *Case C: convergence behavior of the TDOPF and main variables*

1.5.4. *Algorithm performance*

Table 1.7 shows the computational performance of the algorithm in cases A, B and C. The algorithm was run on a common desktop PC (Intel Core i7-4770, 3.40 GHz, 8 GB RAM, 64 bit). The time required for solving each DLF in the derivative numerical evaluation routine is quite small (from 1 to 10 ms). This means that the problem can be solved with a less performant method, accepting the risk of having more iterates before convergence. For this reason, all test cases showed better performances using the simplified Barzilai and Borwein formula, neglecting the line search routine. This is possible as long as the problem is not too complex and the system is supposed to be operating under balanced conditions.

case	num. control resources	num. iteration	total elapsed time [s]	sensitivity evaluation time[s]
A	505	11	11.03	9.82
B	15	9	2.06	2.03
C	15	5	1.03	0.96

Table 1.7. *Case C. Convergence behavior of the TDOPF and main variables*

In the following section, the algorithm will be tested with a full representation of MV and LV circuits, where the hypothesis of balanced load is unfit. The DLF timings necessary for solving LV circuits will require the adoption of more performant solving methods.

1.6. Application of the proposed methodology to the optimization of a MV/LV network

The network model used for tests is based on actual data concerning the MV and LV circuits adopted for primary and secondary distribution in a real urban distribution network in the city of Bari (Italy). Bari is a medium-sized Italian town with approximately 350.000 inhabitants and the area under investigation is only a part of a district counting approximately 60.000 people. The network model developed for tests comprises three whole MV feeders, supplying 22 secondary substations (Figure 1.8). LV circuits start from each MV/LV substation. For instance, a schematic representation of the LV circuits under the substation F1M1 is given in Figure 1.9. Each LV secondary distribution grid has been represented with a 4-wire model. A total number of 590 buses, 2,289 nodes, 576 lines and 24 transformers have been employed for representing the whole system. LV circuits extend for a total length of approximately 23 km. The presence of 21 PV generators with both single-phase and three-phase connections have also been assumed based on real data.

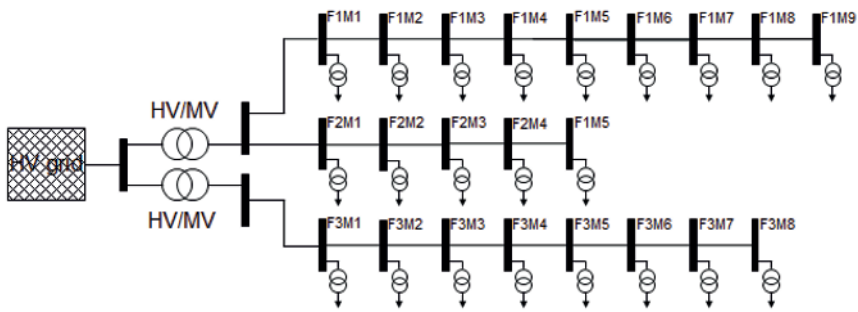

Figure 1.8. *Schematic representation of the 20 kV distribution grid*

Based on aggregated data (number of customers connected to each node), the presence of 2,587 single-phase and 549 three-phase loads have been hypothesized. Single-phase loads have been associated with each phase conductor averaging the load among phases, so that the final load configuration is unbalanced. For each load, a specific ZIP model was assumed [BOK 14]. Having classified all loads into four classes according to their contracted power (residential, small commercial, large commercial and industrial), different ZIP models were associated with each load using a random criteria. The ZIP models and coefficients that have been used are the ones experimentally determined in [BOK 14].

In order to simulate operating conditions, where TDOPF optimization can be applied, some hypothetical operative conditions have been tested.

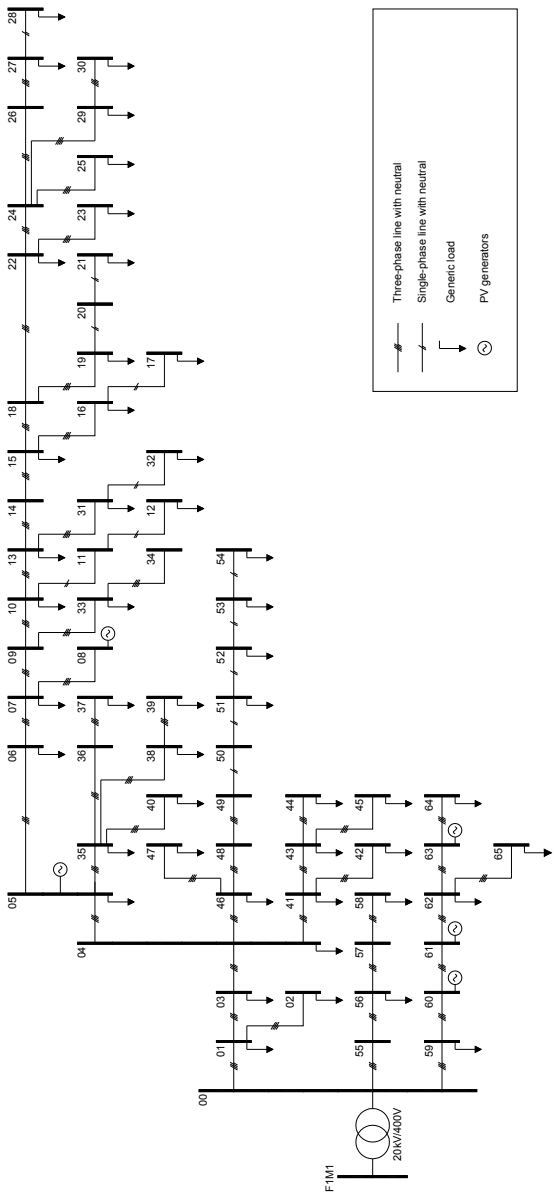

Figure 1.9. *Schematic representation of the 230 V/400 V circuits supplied by the F1M1 substation*

1.6.1. *Case D: LV network congestions*

For this test, the loading level of each LV circuit was set so that the overall demand is 4,050 kW active and 1,990 kVAr reactive power. The 22 MV/LV transformers are rated in the classes 250, 315 and 400 kVA and can supply an overall rated power of 6,910 kVA theoretically. However, feeders and terminal circuits have been loaded, so that three different security problems have arisen altogether. Specifically, the LV distribution circuit in #F1M1 is characterized by currents violating the maximum ampacity, the LV circuit in #F1M4 has voltages violating minimum voltage magnitude constraints, and the MV/LV transformer in #F2M5 is overloaded.

In order to find a new operative state, where all inequality constraints are respected, the availability of a set of active and reactive control resources was assumed. It was assumed that 48 interruptible loads, with a total power capability of approximately 350 kW, are distributed in the system and that the 21 photovoltaic generators can provide regulating reactive power up to half of the produced active power (i.e. a power factor of approximately 0.9) for a total capability of ±166 kVAr.

The control effort required by the available control resources is minimized through the introduction of a cost function that can be formulated as

$$C_0 = \sum_{i=1}^{nctrl} \alpha_{0,i} \left(\frac{u_i - u_i^0}{u_i^{max} - u_i^{min}} \right)^2 \qquad [1.27]$$

where u_i and u_i^0 represent, respectively, the current and the initial value of the *i*-th control variable. For instance, u_i^0 is the amount of load available for curtailment or the initial reactive power supplied by a PV generator (most likely zero).

The coefficient $\alpha_{0,i}$ takes into account the different costs of each control action. For example, reactive control resources can be characterized by a lower (if not null) cost, as they can be considered as cost-free control action. However, in the ideal context of active distribution grids where prosumers (or more generally active users) will be able to sell active and reactive regulating power, $\alpha_{0,i}$ can represent actual bidding of active users.

In this formulation, each resource u_i is constrained by hard constraints as in [1.7]. In the case of curtailable load, u_i^{min} is a positive or null number. A negative

minimum constraint on active control resources might be adopted in the presence of resources that can inject active power (for example, BESS or electric vehicles operating in V2G mode). Hard constraints on reactive control resources are set, so that the power factor for each generator is never lower than 0.9.

In Table 1.8, it is shown how the optimal solution, reached after eight iterations, is characterized by no constraint violations (i.e. all penalty functions are null). This optimal solution is reached by singling-out the control resources characterized by higher sensitivities with respect to the overall function [1.6]. Given the 4-wire model used in the overall formulation, the approach allows treatment of violations on a specific conductor and use of the control resources that are directly connected to that conductor. This is an important feature provided by this method, since any solution based on the sole direct sequence representation of the system is not capable of controlling security violations on single-phase circuits, nor capable of controlling flows and voltages on neutral conductors.

iter #	C_0 [p.u.]	C_1 [p.u.]	C_2 [p.u.]	C_3 [p.u.]	C (tot) [p.u.]
0	0.000	172.100	28.282	1.789	202.171
1	0.065	0.910	14.065	0.023	15.063
2	0.071	0.181	6.904	0.003	7.159
3	0.074	0.046	0.320	0.002	0.442
4	0.077	0.022	0.001	0.002	0.102
5	0.077	0.014	0.000	0.001	0.092
6	0.077	0.003	0.000	0.001	0.081
7	0.077	0.000	0.000	0.000	0.077
8	0.076	0.000	0.000	0.000	0.076

Table 1.8. *Case D1. Algorithm converge behavior*

For instance, the curtailment requested on active control resources under the secondary substation #F1M1 is shown in Figure 1.10. This feeder is characterized by an overload on the three branches from bus F1M1_00 to F1M1_04 (see Figure 1.9). The highest curtailment is requested to loads #1, #2, #3 and #5, which are single-phase loads connected to phase A. Loads #4 and #7 are connected to phase B, and #6 to phase C. Load #8 is connected to phase A but belongs to a different LV feeder that is running parallel to the congested one; no control is requested to this load.

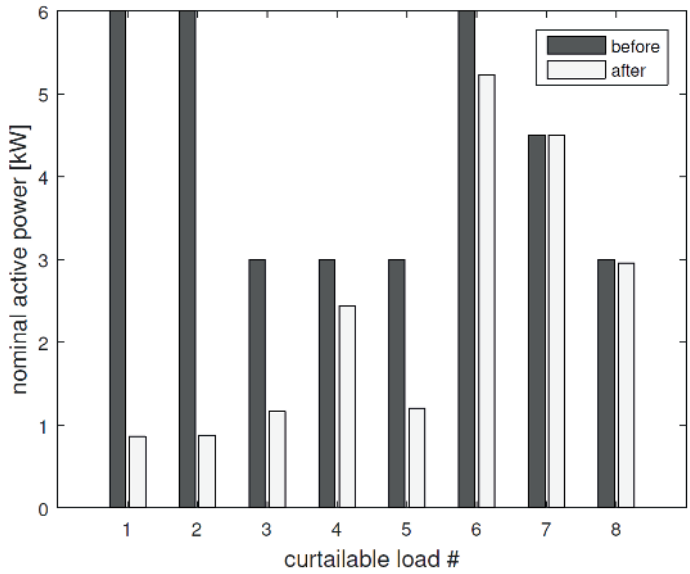

Figure 1.10. *Case D1: Active power supplied to curtailable loads under the secondary substation #F1M1, before and after control*

case	num. active resources	num. reactive resources	active control [ΔkW]	reactive Control [ΔkVAr]
D1	48	21	82.12	7.02
D2	48	0	83.33	0.00
D3	48	63	82.10	27.51

Table 1.9. *Cases D1, D2, D3: active and reactive control*

The solution found is characterized by an overall control of resources of 82.1 kW and 7.0 kVAr. It is possible to run the algorithm neglecting reactive control resources (case D2). The new solution requires the curtailment of approximately 83.3 kW, showing that the contribution of reactive resources is minimum for this specific operative case: the use of non cost-free control actions (load curtailment) cannot be avoided through reactive power rescheduling. This result is also confirmed by case D3, where it was assumed that 42 other distributed reactive resources were available in the network with a total capability of approximately ±50 kVAr. In Table 1.9, where all results are summarized, the overall active and reactive control is expressed as 1-norm of power changes.

Other tests were carried out enabling only reactive control resources. These tests are not represented in Table 1.9 as no feasible solutions were found, even after increasing the number of available control resources. These results are expected given the high R/X ratio that characterizes LV circuits and the scarce control effectiveness that reactive power has in such circuits.

1.6.2. *Case E: minimization of losses and reactive control*

A second test was carried out considering the classical problem of loss reduction. A different operating condition was obtained by decreasing the average power factor of all loads to 0.8 and loading feeders, so that no congestions or voltage violations occur. This case is characterized by losses of 6.60%, calculated with respect to the total load. In order to reduce system losses, an objective function was introduced:

$$C_{loss} = \alpha_{loss} \left(total\ losses \Big/ \sum_{i=1}^{nloads} P_{Li} \right)^2 \qquad [1.28]$$

where P_{Li} is the active power requested by the *i*-th load and α_{loss} is a weight factor.

Reactive control was boosted with respect to case D3, considering that the additional 42 distributed reactive resources have a total capability of approximately ±500 kVAr. The solution of the problem obtained by adding [1.20] in eqn. [1.6], and considering the availability of reactive resources only was reached after few iterations as shown in Table 1.10. With the rescheduling of 144 kVAr, the overall losses were reduced to 6.39%. Two other tests were carried out also considering the availability of active control resources (the same set of curtailable loads available for case A1). Table 1.11 gathers the results of all simulations. In all cases, the algorithm uses reactive power for power factor correction and active power for phase balancing.

iter #	C_0 [p.u.]	C_1+C_2+C_3 [p.u.]	C_{loss} [p.u.]	C (tot) [p.u.]
0	0.000	0.000	4.071	4.071
1	0.000	0.000	4.070	4.070
2	0.002	0.000	3.839	3.841
3	0.003	0.000	3.835	3.838
4	0.003	0.000	3.836	3.839
5	0.003	0.000	3.835	3.838
6	0.003	0.000	3.835	3.838

Table 1.10. *Case E1: algorithm convergence behavior*

case	num. active resources	num. reactive resources	active control [ΔkW]	reactive control [ΔkVAr]	losses [%]
E1	0	63	0.00	144.41	6.39
E2	48	0	132.89	0.00	6.24
E3	48	63	99.21	150.29	6.15

Table 1.11. *Cases E1, E2 and E3: active and reactive control*

1.6.3. *Algorithm performance*

The computational effort required for running the algorithm on a common desktop PC (Intel Core i7-4770, 3.40 GHz, 8 GB RAM, 64 bit) is shown in Table 1.12 for all cases. It can be observed that the algorithm speed is drastically affected by the number of control resources. This is due to the fact that the greatest computational effort is required by the sub-algorithm that evaluates derivatives to compute $\nabla \boldsymbol{C}_{k+1}$ and that the time required for such calculations grows linearly with the number of control variables. Moreover, the time necessary for solving each DLF is approximately 10–100 times higher than that in the previous case (average computation time is more than 100 ms per each DLF routine).

Case	num. control resources	num. iteration	total elapsed time [s]	sensitivity evaluation time[s]
D1	69	8	124.8	120.4
D2	48	8	85.8	81.7
D3	111	8	195.1	190.4
E1	63	6	92.9	85.4
E2	48	7	96.1	79.0
E3	111	9	236.2	225.4

Table 1.12. *Computation time for cases D and E*

In all tests, it was assessed that gradient evaluation requires more than 95% of the overall computing time. For this reason, the most efficient algorithm (BFGS) was adopted.

A simplified formulation, similar to that used in the previous cases, is not suitable for solving this problem. For example, the solution of case D1 with the Barzilai–Borwein method would have required 24 iterations and a 278s running time.

1.7. Conclusions

In this chapter, it has been demonstrated how OPF techniques can be successfully applied in a DMS framework for controlling smart distribution grids at both MV and LV voltage levels. Both centralized and decentralized approaches are viable, as control actions can be based on a direct command to controlled network devices (OLTCs, switched capacitors, disconnectors, etc.) or on the calculation of optimal reference signals or price signals to be sent to prosumers or active end-users.

The development of tools for monitoring and controlling active and reactive power flows and voltages at any voltage level is a required step for the development of smart distribution grids. However, monitoring and control of MV and, especially, LV distribution networks require a substantial leap with regard to the problem of system modeling and inventorying. The classical "fit and forget" approach traditionally used for managing distribution is unfit to accommodate the growing number of distributed active resources.

In this chapter, a methodology for controlling active and reactive resources in LV systems has been proposed. This methodology, based on the solution of a three-phase unbalanced OPF, was tested on a detailed multi-phase representation of actual primary and secondary distribution systems. The formulation is general enough to consider the availability of a wide range of control resources and operational targets.

Test results showed the feasibility of the approach in a DMS framework and showed potential capability of treating large numbers of single-phase and multi-phase power devices.

1.8. Acknowledgments

Concerning developments reported in section 1.5, the authors gratefully acknowledge the Apulia region for financing the project "Smart-Grids: Advanced Technologies for utilities and energy" with 1,133,700 € as a Strategic Project in the Framework Program Agreement on the scientific research sector. Furthermore, the authors would like to thank Mr Walter Leggieri, Technical Director of AMET SpA Power Distribution Company, and all the personnel at the same utility for the help provided during the modeling of the system representation.

Developments reported in section 1.6 are some of the results obtained during the research project PON RES NOVAE (Reti, Edifici, Strade, NuoviObiettivi Virtuosi per l'Ambiente e l'Energia) "Renewable energy and smart grids in smart cities", which was financed with 23,391,010 €. The authors gratefully acknowledge the

Italian Ministry for Education, University and Research and co-financing partners for the research funds under the research and competitiveness program to promote "Smart Cities, Communities and Social Innovation".

1.9. Bibliography

[ABD 12] ABDEL-MAJEED A., BRAUN M., "Low voltage system state estimation using smart meters", *Presented at the 47th International Universities Power Engineering Conference (UPEC)*, London, September 2012.

[ALS 74] ALSAC O., STOTT B., "Optimal load flow with steady-state security", *IEEE Transactions Power Apparatus and Systems*, vol. PAS-93, no. 3, pp. 745–751, 1974.

[BAL 15] BALLANTI A., OCHOA L.F., "Initial assessment of voltage-led demand response from UK residential loads", *Innovative Smart Grid Technologies Conference (ISGT) 2015*, Washington DC, USA, February 2015.

[BAR 88] BARZILAI J., BORWEIN J.M., "Two-point step size gradient methods", *IMA Journal of Numerical Analysis*, vol. 8, pp. 141–148, 1988.

[BAR 95] BARAN M.E., KELLEY A.W., "A branch-current-based state estimation method for distribution systems," *IEEE Transactions Power Systems*, vol. 10, pp. 483–491, 1995.

[BAR 09] BARAN M., MCDERMOTT T.E., " Distribution system state estimation using AMI data", *Presented at the IEEE/PES Power Systems Conference and Exposition 2009 (PSCE'09)*, Seattle, USA, March 2009.

[BAS 15] BASSO T., CHAKRABORTY S., HOKE A. *et al.*, "IEEE 1547 Standards advancing grid modernization", *42nd IEEE Photovoltaic Specialist Conference (PVSC)*, New Orleans, June 2015.

[BOK 14] BOKHARI A., ALKAN A., DOGAN R. *et al.*, "Experimental determination of the ZIP coefficients for Modern Residential, Commercial, and Industrial Loads", *IEEE Transaction Power Delivery*, vol. 29, no. 3, pp. 1372–1381, 2014.

[BRE 97] BREZINSKI C., *Projection Methods for System of Equations*, North-Holland, Amsterdam, 1997.

[BRE 03] BREZINSKI C., "A classification of quasi-Newton methods", *Numerical Algorithms*, vol. 33, pp. 123–135, 2003.

[BRO 11] BRONZINI M., BRUNO S., LA SCALA M. *et al.*, "Coordination of Active and Reactive Distributed Resources in a Smart Grid", *Presented at PowerTech 2011*, Trondheim, June 2011.

[BRU 09] BRUNO S., LA SCALA M., LAMONACA S. *et al.*, "Load control through smart-metering on distribution networks", *PowerTech 2009 Conference*, Bucarest, Romania, June–July 2009.

[BRU 11a] BRUNO S., LA SCALA M., STECCHI U., "Monitoring and Control of a Smart Distribution Network in Extended Real-Time DMS Framework", *Presented at Cigré International Symposium 2011*, Bologna, September 2011.

[BRU 11b] BRUNO S., LAMONACA S., ROTONDO G. *et al.*, "Unbalanced three-phase optimal power flow for smart grids", *IEEE Transactions on Electron Devices*, vol. 58, no. 10, pp. 4504–4513, 2011.

[BRU 12] BRUNO S., LAMONACA S., LA SCALA M. *et al.*, "Integration of optimal reconfiguration tools in Advanced Distribution Management System", *IEEE PES Innovative Smart Grid Technologies Europe 2012*, Berlin, October 2012.

[FAN 09] FAN J., BORLASE S., "The evolution of distribution", *IEEE Power & Energy*, vol. 7, pp. 63–68, no. 2, 2009.

[FAR 14] FARHANGI H., "A road map to integration: perspectives on smart grid development", *IEEE Power Energy Magazine*, vol. 12, no. 3, 2014.

[FIA 83] FIACCO A.V., *Introduction to Sensitivity and Stability Analysis in Nonlinear Programming*, Academic Press, New York, NY, 1983.

[FOR 16] FORFIA D., KNIGHT M., MELTON R., "The view from the top of the mountain: building a community of practice with the GridWise Transactive Energy Framework", *IEEE Power and Energy Magazine*, vol. 14, no. 3, pp. 25–33, 2016.

[HAD 10] HADJSAID N., LE-THANH L., CAIRE R. *et al.*, "Integrated ICT framework for distribution network with decentralized energy resources: Prototype, design and development", *IEEE PES General Meeting 2010*, Minneapolis, 25–29 July 2010.

[HTT] https://sourceforge.net/projects/electricdss/

[KRI 16] KRISTOV L., DE MARTINI P., TAFT J.D., "A tale of two visions: designing a decentralized transactive electric system", *IEEE Power and Energy Magazine*, vol. 14, no. 3, pp. 63–69, 2016.

[LU 95] LU C.N., TENG J.H., LIU W.H.E., "Distribution system state estimation," *IEEE Transaction Power System*, vol. 10, pp. 229–240, 1995.

[MAL 14] MALLET P., GRANSTROM P.-O., HALLBERG P. *et al.*, "Power to the People!: European perspectives on the future of electric distribution", *IEEE Power Energy Magazine*, vol. 12, no. 2, pp. 51–64, 2014.

[MEL 11] MELIOPOULOS A.P.S., COKKINIDES G., HUANG R. *et al.*, "Smart grid technologies for autonomous operation and control", *IEEE Transaction on Smart Grid*, vol. 2, no. 1, 2011.

[MOH 10] MOHAGHEGHI S., STOUPIS J. *et al.*, "Demand response architecture: integration into the distribution management system", *1st IEEE International Conference on Smart Grid Communication (SmartGridComm)*, 2010, Gaithersburg, MD, October 2010.

[MOK 13] MOKHTARIA G., NOURBAKHSHA G., ZAREB F., *et al.*, "Overvoltage prevention in LV smart grid using customer resources coordination", *Energy and Buildings*, vol. 61, pp. 387–395, 2013.

[MOM 09] MOMOH J.A., "Smart grid design for efficient and flexible power networks operation and control", *IEEE – Power Systems Conference and Exposition 2009*, Seattle, March 2009.

[MOR 79] MORGAN M.G., TALUKDAR S.N., "Electric power load management: Some technical, economic, regulatory and social issues", *Proceedings of the IEEE*, vol. 67, no. 2, pp. 241–312, 1979.

[NOC 06] NOCEDAL J., S.J., *Numerical Optimization*, Springer, New York, 2006.

[PAU 11] PAUDYAL S., CANIZARES C., BHATTACHARYA K., "Optimal operation of distribution feeders in smart grids", *IEEE Transaction on Industrial Electronics*, vol. 58, no. 10, pp. 4495–4503, 2011.

[RAH 16] RAHIMI F., IPAKCHI A., FRED FLETCHER F., "The changing electrical landscape: end-to-end power system operation under the transactive energy paradigm", *IEEE Power and Energy Magazine*, vol. 14, no. 3, pp. 52–62, 2016.

[ROY 93] ROYTELMAN I., SHAHIDEHPOUR S.M., "State estimation for electric power distribution systems in quasi real-time conditions", *IEEE Transaction Power Delivery*, vol. 8, no. 4, pp. 2009–2015, 1993.

[SAN 10] SANTACANA E., RACKLIFFE G., TANG L., *et al.*, "Getting smart", *IEEE Power & Energy*, vol. 8, pp. 41–48, no. 2, 2010.

[SIN 09] SINGH R., PAL B.C., JABR R.A., "Choice of estimator for distribution system state estimation", *IET Generation, Transmission & Distribution*, vol. 3, no. 7, pp. 666–678, 2009.

[SMA 16] SMART ENERGY DEMAND COALITION (SEDC), Report on "Mapping Demand Response in Europe Today – 2015", available at: http://www.smartenergydemand.eu/, 2016.

[STI 11] STIFTER M., BLETTERIE B., BURNIER D. *et al.*, "Analysis environment for low voltage networks", *2011 IEEE 1st Int. Workshop on Smart Grid Modeling and Simulation (SGMS)*, Brussels, October 2011.

[STI 13] STIFTER M., PALENSKY P., "Smart meter data as a basis for smart control in low voltage distribution networks", *2013 IEEE Int. Symposium on Industrial Electronics (ISIE)*, Taipei, May 2013.

[TIN 68] TINNEY W.F., HART C.E., "Optimal power flow solutions", *IEEE Transaction Power Apparatus and Systems*, vol. PAS-87, pp. 1886–1876, 1968.

[VAR 15] VARELA J., PUGLISI L.J., WIEDEMANN T. *et al.*, "Show Me!: large-scale smart grid demonstrations for European distribution networks", *IEEE Power Energy Magazine*, vol. 3, no. 1, pp. 85–91, 2015.

[WAN 04] WANG H., SCHULZ N.N., "A revised branch current based distribution system state estimation algorithm and meter placement impact", *IEEE Transaction Power System*, vol. 19, no. 1, pp. 207–213, 2004.

[ZHA 10] ZHAO L., ZHENYUAN W. *et al.*, "A unified solution for advanced metering infrastructure integration with a distribution management system", *1st IEEE International Conference on Smart Grid Communication (SmartGridComm)*, 2010, Gaithersburg, MD, October 2010.